CHAPTER III

EXPERIMENTAL BACKGROUND AND CHARACTERIZATION METHOD

In this chapter, we inform the growth information of GaAsN thin films (bulk layer) and GaAsN/GaAs MQWs. Subsequently, the basic understanding of structural and optical characterization is described.

3.1 Preparation of GaAsN Alloy Samples

All samples used in this work, including the $GaAs_{1-x}N_x$ alloy films and the $GaAs_{1-x}N_x$/GaAs QWs were prepared at Prof. Dr. Kentaro Onabe's laboratory, The University of Tokyo, Japan.

3.1.1 MOVPE Growth Information of GaAsN Bulk Layers

$GaAs_{1-x}N_x$ layers with N contents (x) of $x = 0.015$ and $x = 0.051$ were grown on GaAs (001) substrates without cap layer by metalorganic vapor phase (MOVPE) using trimethylgallium (TMGa), 1, 1-dimethylhydrazine (DMHy), and tertiarybutylasine (TBAs) as the source materials for Ga, N, and As, respectively. The DMHy (N) flow rates were 1,500 and 5,000 μmol/min for the N contents of $x = 0.015$ and $x = 0.051$, respectively. In order to improve the luminescence intensity, the post-growth thermal annealing was performed in the growth reactor at 650°C for 2 min and 5 min under TBAs and H_2 ambient [14].

3.1.2 MOVPE Growth Information of GaAsN/GaAs MQWs

The $GaAs_{0.950}N_{0.050}$/GaAs MQWs structures with the GaAs barriers and the $GaAs_{0.950}N_{0.050}$ well layers were grown on the GaAs (001) substrate by MOVPE using trimetylgallium (TMGa), tertiarybutylarsine (TBAs) and 1, 1-dimethylhydrazine

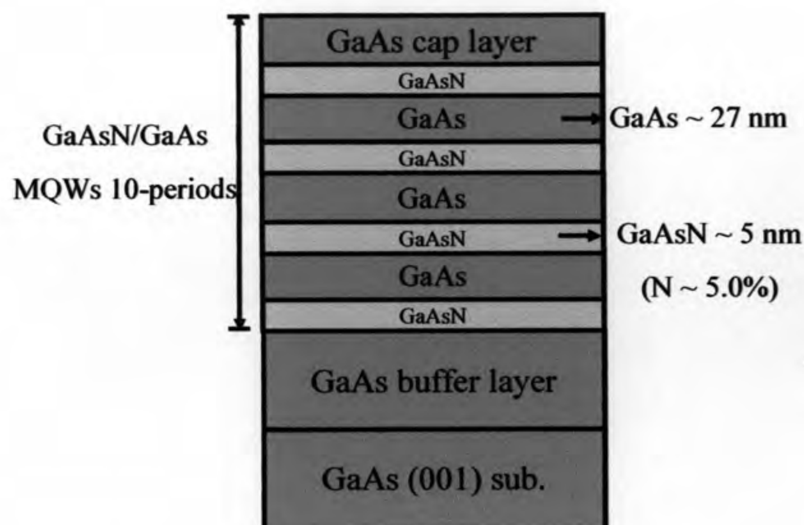

Figure 3.1: Schematic diagram of GaAsN/GaAs 10-periods MQWs.

(DMHy) as the source materials for Ga, As and N, respectively. Note that the growth conditions for the $GaAs_{0.950}N_{0.050}$ well layers were similar to the growth conditions for the $GaAs_{0.949}N_{0.051}$ bulk sample. First, a 600 nm-thick GaAs buffer layer was grown, followed by a strained $GaAs_{0.950}N_{0.050}$ well layer. The GaAsN/GaAs MQWs consists of 10-periods GaAsN well and GaAs barrier layers to improve the optical efficiency. Sample structure of the GaAsN/GaAs MQWs is shown in Fig. 3.1. Thicknesses of the well and barrier layers were examined to be 5.0 and 26.0 - 27.0 nm, respectively.

To improve the luminescence intensity of the $GaAs_{0.950}N_{0.050}$/GaAs MQWs, the post-growth thermal annealing was also performed at 650°C for 2 min under TBAs and H_2 ambient [14].

3.2 Structural Characterization

High-resolution X-ray Diffraction

High-resolution X-ray diffraction (HRXRD) is widely used to investigate the structural properties and crystal quality of the epitaxial semiconductor films and their

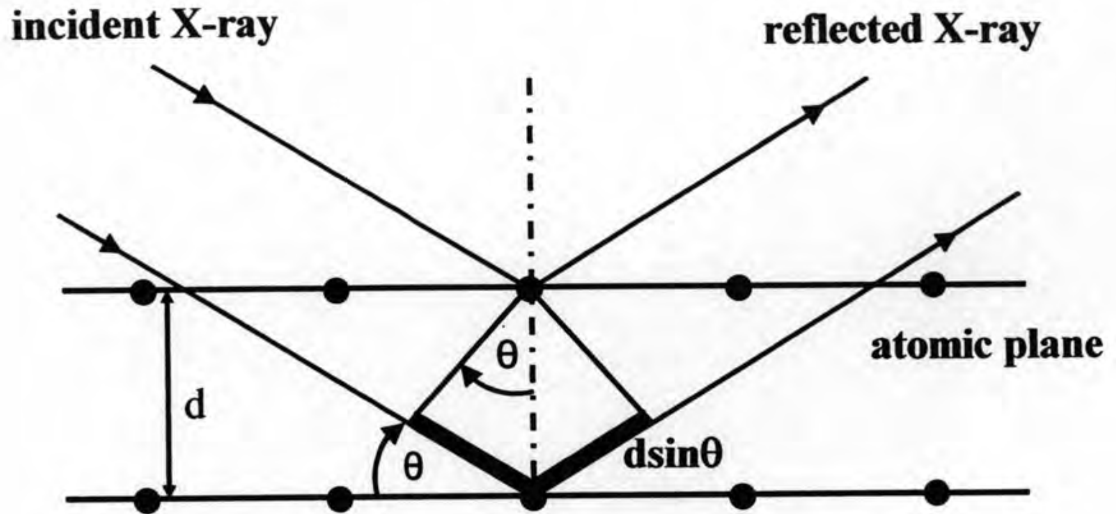

Figure 3.2: Schematic diagram of Bragg's law.

QW structures, such as the lattice parameters, alloy composition and strain properties. When parallel X-rays strike a pair of parallel lattice planes, every atom within the planes acts as a scattering center and reflects a secondary wave, as shown in Fig. 3.2. All of the secondary waves combine to form a reflected wave. The same occurs on the parallel lattice planes with the lattice plane distance of d_{hkl}. All these reflected waves interfere with each other and obey Bragg's law.

$$2d_{hkl}\sin\theta = n\lambda. \quad (3.1)$$

For a defined incident X-ray wavelength (λ) and a defined lattice plane distance (d_{hkl}), the Eq. (3.1) is only given with a specific angle. In this work, the incident X-ray wavelength (λ) of 1.5406 Å is used. In the case of strained epitaxy, the layer distorts along the growth direction to produce a tetragonal distortion. The value of d_{hkl} can be represented as follow,

$$d_{hkl} = \frac{a_{//}}{\sqrt{h^2+k^2}} + \frac{a_{\perp}}{\sqrt{l^2}}. \quad (3.2)$$

It is well known that, with incorporation of N, the GaAsN layer grown on the GaAs substrate is under tensile strain, as shown in Fig. 3.3. In order to analyze the lattice parameters ($a_{//}$ and $a_{\perp}$), both symmetric (004) and asymmetric (115) reflections were

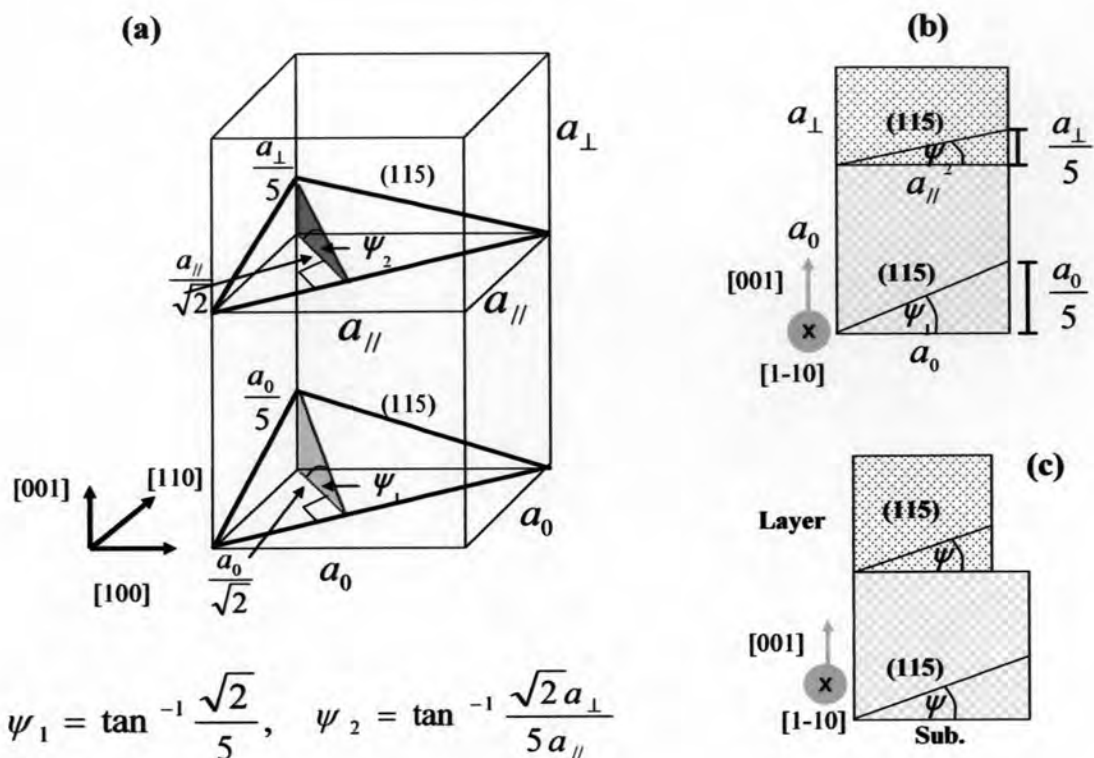

Figure 3.3: (a) Three dimensional lattice structure under tensile strain, (b) and (c) two dimensional lattice structures of tensile strained and fully relaxed layers, respectively.

measured by the (004) $2\theta/\omega$-scan and the (115) $\Delta(\omega)$ and $\Delta(2\theta/\omega)$ reciprocal space mapping.

In this work, HRXRD measurements were done at Department of Advanced Material Science, The University of Tokyo and at Scientific and Technological Research Equipment Center, Chulalongkorn University (Bruker-AXS D8 DISCOVER). The HRHRD measurements were performed using a copper target ($K\alpha_1$ = 1.5406 Å) as the radiation source.

Determination of Lattice Constant

The symmetric (004) $2\theta/\omega$-scan was performed to examine the normal plane ($a_\perp$) of strained GaAsN layers. For an example, Fig. 3.4 shows a HRXRD (004) $2\theta/\omega$ scan of the strained GaAsN layer on GaAs (001) substrate. From the separation between the GaAs and GaAsN reflection peaks, $a_\perp$ can be calculated using Bragg's

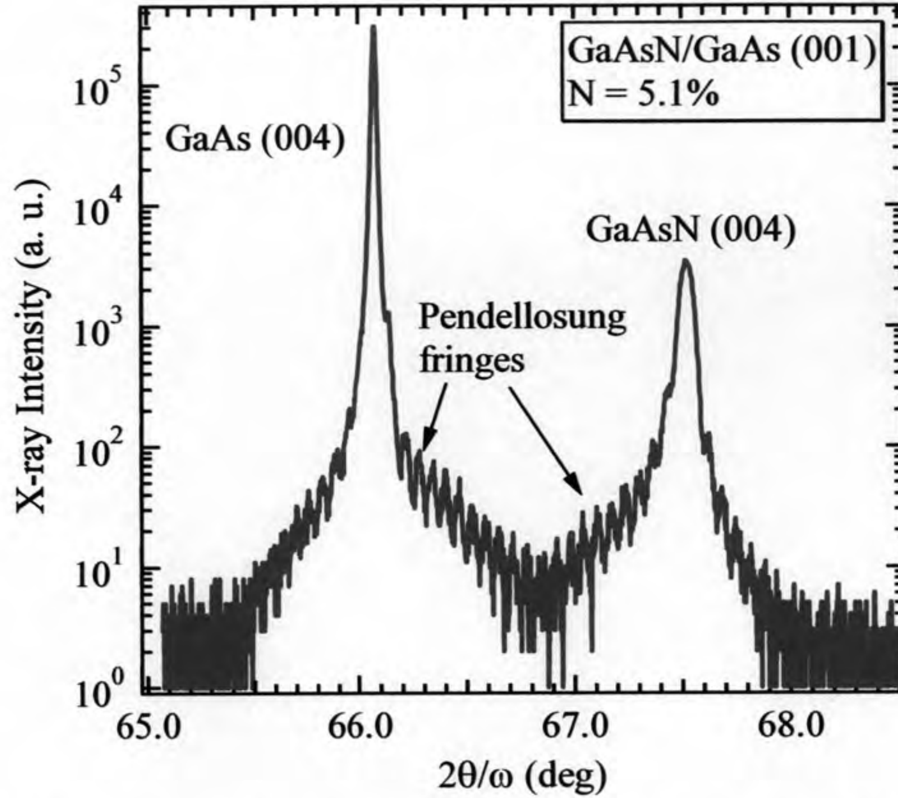

Figure 3.4: Symmetrical (004) HRXRD *2θ/ω* curve of the as-grown $GaAs_{0.949}N_{0.051}$ layer.

law, Eq. (3.1). In addition, the thickness of the GaAsN layer can be calculated from the separation of Pendellösung fringes by using standard formula [37]. To determine the in-plane lattice parameter ($a_{//}$) of strained GaAsN layer, the asymmetric (115) $\Delta(\omega)$ - $\Delta(2\theta/\omega)$ reciprocal space mapping technique was performed. In the strained layer, it is known that the inclination between the asymmetric plane of substrate and that of the epitaxial layer is commonly observed owing to tetragonal distortion, as shown in Fig. 3.3. The angle (ψ) between the (001) plane and (115) of the strained layer is given by [38]

$$\psi = \tan^{-1}(\sqrt{2} \cdot a_{\perp} / 5 \cdot a_{//}). \tag{3.3}$$

For the fully relaxed layer ($a_{epi} = a_{//} = a_{\perp}$) such as GaAs substrate, thus, ψ becomes a constant value of $\tan^{-1}(\sqrt{2}/5)$. Due to the tetragonal lattice distortion of the strained

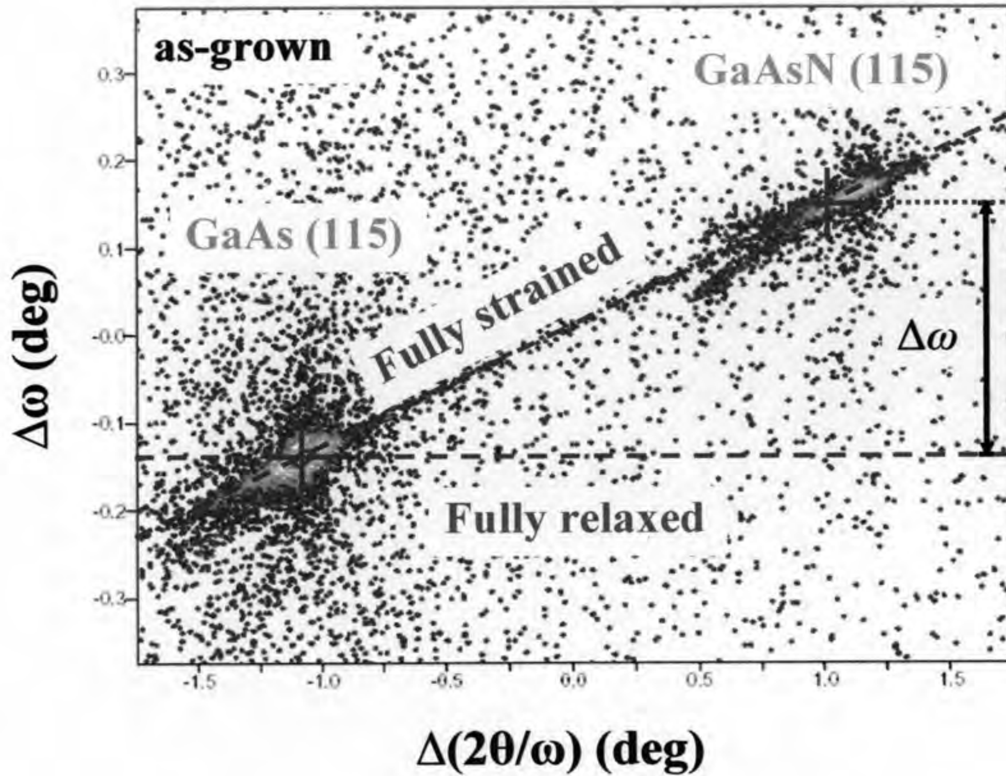

Figure 3.5: Asymmetric (115) reciprocal lattice map of the as-grown $GaAs_{0.949}N_{0.051}$ layer.

GaAsN layer ($a_{//} \neq a_{\perp}$), the tilted angle $\Delta\psi$ between the GaAs (115) and GaAsN (115) planes is represented by [38]

$$\Delta\psi \equiv \psi_{GaAs} - \psi_{GaAsN} = \tan^{-1}(\sqrt{2}/5) - \tan^{-1}(\sqrt{2} \cdot a_{\perp}/5 \cdot a_{//}). \qquad (3.4)$$

Assume that the GaAs substrate is fully relaxed.

In the experiment set up, the value of ω indicates a combination of the incident angle θ and the inclination angle (offset angle) between sample and stage holder of the instrument set up. Thus, for the fixed value of 2θ, the value of $\Delta\omega$ is equivalent to the tilted angle ($\Delta\psi$) between the (001) plane and (115) of the strained layer. Therefore, the high-resolution $\Delta\omega$ -$\Delta(2\theta/\omega)$ mapping technique can be applied to determine both the tilted angle $\Delta\psi$ and actual Bragg angle of the grown layer. In addition, the mosaic structure within the layers can also be observed.

In an example case, Fig. 3.5 shows a typical ω-scan and $2\theta/\omega$-scan mapping measured around the asymmetric (115) reflection. In Fig. 3.5, the fully relaxed and

fully strained lines represent the unstrained and strained GaAsN layer. If the GaAsN (115) peak is at the fully strained line, it will be indicated that the in-plane lattice constant of the GaAsN layer is in agreement with a lattice constant of GaAs substrate. Figure 3.5 shows that the GaAsN (115) peak is at the fully strained line corresponding to the fully strained layer. If the GaAsN (115) peak is between the fully strained and fully relaxed lines, it will be suggested that the layer is a partially relaxed layer. The separation between GaAs and GaAsN peaks in ω-axis, which corresponds to the tilted angle $\Delta\psi$ ($\Delta\psi = \Delta\omega$ in Fig. 3.5) between GaAs (115) and GaAsN (115) planes, the $a_{//}$ can be calculated by Eq. (3.4.). The HRXRD mapping measurement is a practical method to determine the precise lattice parameters of the coherently strained layer as well as the partially relaxed layers.

Examination of N Concentration

From an elastic deformation of epitaxial films the lattice constant of the relaxed $GaAs_{1-x}N_x$ lattice, a_0, is calculated according to [38]

$$a_0 = \frac{2C_{12}a_{//} + C_{11}a_{\perp}}{2C_{12} + C_{11}}, \tag{3.5}$$

where C_{11} and C_{12} are the elastic constants of $GaAs_{1-x}N_x$ alloy. The N composition (x) is estimated from a_0 assuming Vergard's law

$$a_0 = x \cdot a_{c-GaN} + (1-x) \cdot a_{GaAs}, \tag{3.6}$$

$$C_{11} = \frac{x \cdot a_{c-GaN} C_{11}^{c-GaN} + (1-x) \cdot a_{GaAs} C_{11}^{GaAs}}{a_0}, \tag{3.7}$$

$$C_{12} = \frac{x \cdot a_{c-GaN} C_{12}^{c-GaN} + (1-x) \cdot a_{GaAs} C_{12}^{GaAs}}{a_0}. \tag{3.8}$$

หอสมุดกลาง ศูนย์วิทยทรัพยากร
จุฬาลงกรณ์มหาวิทยาลัย

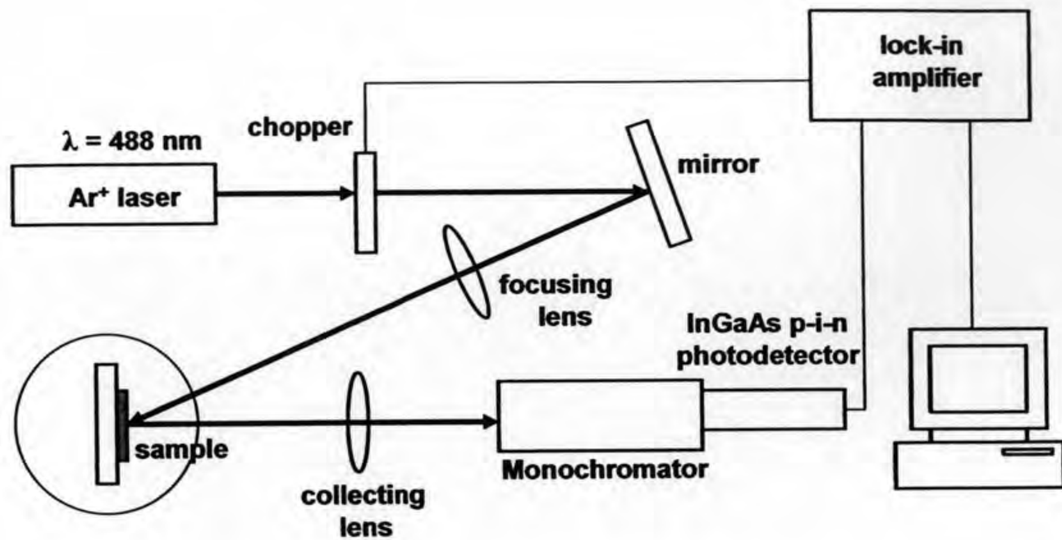

Figure 3.6: Schematic diagram of PL instrument set up

These four equations (Eqs. 3.5 – 3.8) were used to determine the N concentration (x) in the $GaAs_{1-x}N_x$ layer. For the strained layer, both $a_\perp$ and $a_{//}$ have to be determined from the (004) $2\theta/\omega$ scan and the (115) $\Delta\omega$ -$\Delta(2\theta/\omega)$ mapping, respectively. First, we assume that an elastic constant of the dilute GaAsN is equal to that of GaAs. After that the N concentration (x) is calculated from Vergard's law (Eq. 3.6). Next, the values of C_{11} and C_{12} of $GaAs_{1-x}N_x$ were obtained by substituting of the calculated value of x into Eqs. (3.7) and (3.8). To obtain more accurate value of x, we repeated the entire calculation until the difference between input and output composition was much smaller than the error bars (0.001%), which were obtained from the measurement conditions.

3.3 Optical Characterization

In this thesis, the optical properties of GaAsN alloy are investigated by the photoluminescence (PL) measurement. In PL spectroscopy, a light source is used for excitation to create electron-hole pairs. The energy of excited photon is not smaller than the bandgap energy of the sample. Emission of light from a semiconductor is the result of recombination of an electron and a hole. The wavelength of the light is determined by the energy difference between the recombining electron and hole states. By analyzing the emitted light, we can obtain information about the energy levels

such as impurity levels and defect related states, recombination mechanisms and material quality.

Low-temperature (< 10 K) PL measurement is usually used to study the lowest transition energy state in semiconductor. At low-temperature the created electrons and holes are recombined at the lowest transition energy states. In general, the radiative recombination in pure semiconductors is between states in the conduction band and valence band, with the energy difference being known as the bandgap energy. Conversely, the radiative transition in impure semiconductors is between states in the localized states and valence bands, the PL peak energy associated with these levels. It is noted that the informed radiative recombination from the low-temperature PL for impure semiconductors is not enough to know the transition energy states or bandgap energy in the materials. Thus, temperature dependent PL measurement was performed.

Temperature dependent PL measurement can be performed by varying temperature of the sample. The changes of PL spectra at any temperature can be used to obtain the more detail of the mechanism recombination corresponding to the transition energy states in the material.

In this work, the 488 nm line of an Ar^+ laser was used as an excitation light source for the PL measurement. The luminescence was dispersed by a 0.3 m monochromator, and detected by InGaAs p-i-n photodetector using the conventional lock-in technique. The PL set up is shown in Fig. 3.6. The temperature dependent PL measurements were performed at various temperatures ranging from 10 K to 300 K. All PL data were recorded and obtained from Prof. Dr. Kentaro Onabe's laboratory, The University of Tokyo.